

# UCSF

## UC San Francisco Previously Published Works

### Title

Update on Imaging-Based Measurement of Bone Mineral Density and Quality

### Permalink

<https://escholarship.org/uc/item/0fd4g08x>

### Journal

Current Rheumatology Reports, 22(5)

### ISSN

1523-3774

### Authors

Link, Thomas M  
Kazakia, Galateia

### Publication Date

2020-05-01

### DOI

10.1007/s11926-020-00892-w

Peer reviewed



Published in final edited form as:

*Curr Rheumatol Rep.* ; 22(5): 13. doi:10.1007/s11926-020-00892-w.

## Update on Imaging-Based Measurement of Bone Mineral Density and Quality

Thomas M. Link<sup>1</sup>, Galateia Kazakia<sup>1</sup>

<sup>1</sup>Department of Radiology, University of California, 400 Parnassus Ave, A-367, San Francisco, CA 94143, USA

### Abstract

**Purpose of Review**—Patients with inflammatory arthropathies have a high rate of fragility fractures. Diagnostic assessment and monitoring of bone density and quality are therefore critically important. Here, we review standard and advanced techniques to measure bone density and quality, specifically focusing on patients with inflammatory arthropathies.

**Recent Findings**—Current standard procedures are dual-energy X-ray absorptiometry (DXA) and quantitative computed tomography (QCT). DXA-based newer methods include trabecular bone score (TBS) and vertebral fracture assessment (VFA). More advanced imaging methods to measure bone quality include high-resolution peripheral quantitative computed tomography (HR-pQCT) as well as multi-detector CT (MD-CT) and magnetic resonance imaging (MRI). Quantitative ultrasound has shown promise but is not standard to assess bone fragility.

**Summary**—While there are limitations, DXA remains the standard technique to measure density in patients with rheumatological disorders. Newer modalities to measure bone quality may allow better characterization of bone fragility but currently are not standard of care procedures.

### Keywords

Osteoporosis; Bone fragility; Inflammatory arthropathies; Bone mineral density; Bone quality; DXA

### Introduction

Rheumatic diseases are very frequently associated with significant bone loss related to the inflammatory disorder itself, therapies that induce bone loss—in particular corticosteroids—and reduced physical activity. Fragility fractures are therefore frequently observed in rheumatic diseases. Optimal management includes measurement of bone density and quality to diagnose fracture risk and monitor osteoporosis-specific therapies. Bone loss found in rheumatoid arthritis, for example, results in an increased risk of osteoporotic fractures in all

---

Thomas M. Link, Thomas.Link@ucsf.edu.

**Conflict of Interest** The authors declare that they have no conflict of interest.

**Human and Animal Rights and Informed Consent** This article does not contain any studies with human or animal subjects performed by any of the authors.

**Publisher's Note** Springer Nature remains neutral with regard to jurisdictional claims in published maps and institutional affiliations.

age groups, men and women, as well as various anatomic sites compared with controls with an overall relative risk of 2.25 (95% CI 2.25–3.83) [1•].

This review article will focus on standard and advanced techniques to measure bone density and quality in patients with inflammatory rheumatological arthropathies. We will cover dual-energy X-ray absorptiometry (DXA), including trabecular bone score (TBS), quantitative computed tomography (QCT), quantitative ultrasound (QUS), high-resolution peripheral quantitative computed tomography (HR-pQCT), multi-detector CT (MD-CT), and magnetic resonance imaging (MRI) as well as advanced technologies to analyze bone quality using volumetric datasets.

## Specific Considerations for Measuring Bone Mineral Density and Quality in Rheumatic Diseases

In inflammatory arthropathies, pro-inflammatory cytokines are responsible for osteoclast activation, stimulating bone resorption while simultaneously suppressing bone formation [2•]. This is particularly pronounced in the joints and typically associated with synovial hyperplasia. Eventually, this leads to periarticular osteopenia and erosive bone changes. Juxtaarticular osteopenia tends to be more severe in rheumatoid arthritis than in other inflammatory arthropathies such as psoriatic arthritis.

Systemic bone loss is driven by chronic systemic inflammation, reduced physical activity, and anti-inflammatory medications especially glucocorticoids [3]. Interestingly, however, glucocorticoids induce rapid bone loss and a significant increase in fracture risk, particularly fractures of the vertebral bodies, which cannot be fully explained by any decrease in BMD measured with DXA [4]. Measures of bone structure and marrow composition have therefore been proposed to better characterize fracture risk in patients with glucocorticoid therapy [4, 5].

DXA also has limitations in patients with ankylosing spondylitis (AS), in particular in advanced disease where measurements of the spine in the anteroposterior projection are not reliable and may give falsely elevated results due to syndesmophyte formation and ligamentous ossifications [6]. Alternative methods have been proposed to measure bone strength in these patients including HR-pQCT [6, 7]. Similar issues have been found with advanced degenerative disease of the spine and diffuse idiopathic skeletal hyperostosis (DISH), where QCT may be preferable to DXA to measure fracture risk [8].

## Diagnostic Techniques to Measure Bone Mineral Density

### Dual-Energy X-ray Absorptiometry

Currently, DXA is the standard technique to measure bone mineral density. The most frequently used measurement sites are the proximal femur, the lumbar spine, and the distal radius. The measurements have a low radiation dose (effective dose adult spine DXA 0.013 mSv and hip DXA 0.009 mSv compared with a lumbar spine radiograph 0.7 mSv [9]). DXA measurements also have a low precision error (short-term precision spine 1.3%, total hip 1.2%, and femoral neck 1.4%) [10].

For many years, DXA has been the standard to define osteoporosis and osteopenia [11]; this definition is based on T-scores, which compare the BMD of an individual with a young normal reference population. A T-score of  $-2.5$  and lower, i.e., 2.5 or more standard deviations below a young normal reference population, is defined as osteoporosis, while a T-score between  $-1.1$  and  $-2.4$  is defined as osteopenia. A T-score of  $-1.0$  and higher is considered normal. Reference populations are specific to gender and race, and reference data are built into the DXA analysis software from information entered by the technologist performing the test. The World Health Organization (WHO) definition originally applied only to postmenopausal women but according to the International Society of Clinical Densitometry (ISCD) guidelines, these definitions may also be used for men older than 50 [12-14]. Figure 1 shows a DXA spine image of a patient with rheumatoid arthritis and BMD in the osteoporotic range. In addition, the ISCD has introduced guidelines for DXA of premenopausal women, men younger than 50, and children [12-14]. In these populations, Z-scores are used which compare individual BMD measurements with age-matched reference populations; a Z-score lower than  $-2$  is defined as “bone mineral density below the expected range for age”. In these younger populations, the terms osteopenia or osteoporosis are not used to classify BMD measurements.

DXA is also used for monitoring therapy. The least significant change that can be measured directly depends on the precision error [15]. In general, using DXA of the spine and hip, a change in BMD of approximately 5% shows a therapy effect.

It should also be noted that DXA has a number of limitations that need to be considered. Since DXA measures BMD in a projectional image, the measurement is sensitive to degenerative changes of the spine and overlying structures such as aortic calcification, which will result in an overestimation of BMD, especially in older men but also in patients with AS and extensive syndesmophytes. Moreover, because density measurements are areal, BMD will be underestimated in patients who are small and overestimated in patients who are tall. Further, due to its projectional nature, DXA cannot differentiate trabecular from cortical BMD. This can be problematic when trying to detect compartment-specific bone changes common in patients with rheumatological disorders, for example, glucocorticoid-induced cortical porosity. Recently, however, DXA-based techniques have been developed that allow to differentiate trabecular and cortical compartments in DXA image datasets. These are based on statistical 3D shape and density models of the proximal femur built from a database of QCT scans, which are registered to hip DXA scans [16, 17].

Several large studies have shown that DXA BMD measurements have limitations in differentiating patients with and without prevalent vertebral fractures, in predicting new fragility fractures, and in monitoring therapy [18-21]. For example, Siris et al. showed in 149,524 white postmenopausal women aged 50–104 years using peripheral DXA measurements that 82% of the women with new fragility fractures had T-scores higher than  $-2.5$  [21].

Given these limitations of DXA BMD, the FRAX® fracture risk assessment tool (<http://www.sheffield.ac.uk/FRAX/>) [22-24] was developed, which incorporates femoral neck BMD and additional clinical risk factors such as therapy with glucocorticoids, history of

rheumatoid arthritis, previous fracture, fractured hip of a parent, as well as current smoking, alcohol, and secondary osteoporosis. FRAX® provides a 10-year probability risk of a hip or major osteoporosis-related fracture. In patients who are osteopenic, osteoporosis-specific therapy is recommended if the hip fracture risk is  $\geq 3\%$  or the risk of a major fracture is  $\geq 20\%$  [25]. FRAX is generally not used if BMD is normal or if patients have osteoporotic BMD.

The ISCD official positions from 2019 ([www.iscd.org/official-positions/2019-iscd-official-positions-adult/](http://www.iscd.org/official-positions/2019-iscd-official-positions-adult/)) provide detailed information on indications for BMD testing, which include age 65 and older in women and 70 and older in men. In younger patients, BMD testing is recommended if the patients have risk factors for low bone mass such as prior fracture, high-risk medication, and diseases associated with bone loss. The American College of Radiology (ACR) Appropriateness Criteria on osteoporosis and bone mineral density also include rheumatoid arthritis and other inflammatory arthritides as indications for BMD measurements in premenopausal women and men 20–50 years of age [26].

## Trabecular Bone Score

Given the limitations of bone density measurements, researchers have developed tools to assess not simply density but measures of bone architecture. Most of these efforts have focused on volumetric methods based on high-resolution CT or MRI, but low-cost alternatives have also been investigated. Thus, researchers have used standard (projectional) DXA images of the lumbar spine and calculated measures of gray-level texture to define a trabecular bone score (TBS) [27]. TBS uses the gray value of each pixel as well as the information on the degree of spatial dependency for each pixel and its neighboring pixels to extract for each vertebra a variogram as the sum of the squared gray-level differences between pixels at a specific distance. TBS (unitless) is then calculated as the slope of the log-log transform of this variogram with the slope representing the rate of gray-level amplitude variations [28].

A high number of pixel-gray value variations and therefore a steep variogram slope with a high TBS value are found in dense trabecular bone structure, while more porous, osteoporotic trabecular bone produces a low TBS value [28, 29]. TBS reports provide unitless values for the L1-4 vertebra separately and for the total lumbar spine. As with BMD measurements, abnormal or fractured vertebrae are excluded from the analysis. A number of clinical studies demonstrated that low TBS values were associated with increased prevalence and incidence of fragility fractures in postmenopausal women and in older men [30-33] and that the predictive ability of TBS was independent of clinical risk factors, FRAX, and DXA BMD [30]. According to McCloskey, a TBS of  $> 1.31$  is considered normal bone, 1.23 to 1.31 is partially degraded, and  $< 1.23$  is degraded bone [34].

TBS is also included in the ISCD official positions from 2019 ([www.iscd.org/official-positions/2019-iscd-official-positions-adult/](http://www.iscd.org/official-positions/2019-iscd-official-positions-adult/)) stating its association with vertebral, hip, and major osteoporotic fractures in postmenopausal women and men over 50 years. However, there are clear recommendations not to use TBS alone for treatment recommendation, and the role of TBS in monitoring antiresorptive therapy is unclear. A recent scientific article

investigated clinical variables to find out which patients might experience the greatest benefit from TBS measurements [35]; among these were glucocorticoid use and to a lesser extent rheumatoid arthritis. Another study found that in patients with rheumatoid arthritis, TBS measured at the lumbar spine had a better discrimination value than lumbar spine BMD, and similar to femoral neck BMD, in differentiating patients with and without vertebral fractures [36].

### **Vertebral Fracture Assessment and Detection of Atypical Fractures**

It should be noted that DXA has also been used as a diagnostic and not quantitative method by using the same machine to create images to detect and semiquantitatively assess vertebral fractures and to document atypical femur fractures related to osteoporosis therapy. Vertebral fracture assessment (VFA) is typically performed to diagnose asymptomatic vertebral fractures and the scans cover the entire thoracic and lumbar spine. VFA studies may be particularly useful in people with rheumatic diseases, particularly in rheumatoid arthritis and AS, in whom vertebral fractures are frequently found [37].

The official positions of the ISCD for detection of atypical fractures have recently been published [38]. Different DXA imaging algorithms have been described to image the femora to look for focal periosteal and endosteal thickening as well as the presence of a stress fracture (lucent) line at the lateral cortex.

### **Quantitative CT**

QCT was developed for BMD measurements prior to DXA and though it is currently much less frequently used than DXA, it has some pertinent advantages over DXA. Most importantly, QCT allows true volumetric measurements of the lumbar spine and proximal femur, which are independent of body size, and QCT is able to separate trabecular and cortical compartments. It has been shown previously that compartment-specific measurements are more sensitive to therapy than combined trabecular/cortical measurements as in DXA [39]. But there are also some notable disadvantages of QCT, which include the higher radiation dose (0.06–2.9 mSv) [9].

QCT is typically performed at the lumbar spine (L1-3) and the proximal femur. At the spine, single slice or volumetric techniques are used, covering a mid-vertebral region or the entire vertebral body. Exams are mostly performed with calibration phantoms, which allow the conversion from Hounsfield units into mg hydroxyapatite/cm<sup>3</sup> (Fig. 2). More recently, phantomless acquisition methods are available that use fat and muscle for calibration. To interpret the quantitative measurements, absolute BMD values and not T-scores are used, according to the American College of Radiology Practice Parameter for the Performance of Musculoskeletal Quantitative Computed Tomography (Revised 2018 version). (The American College of Radiology will be abbreviated ACRad to distinguish it from the American College of Rheumatology.) A BMD value above 120 mg/ml is defined as normal BMD, 80–120 mg/ml as osteopenia, and below 80 mg/ml as osteoporosis. For the hip, the 3D measurements are transformed into 2D measurements (CTXA) analogous to the hip DXA image and given the similarity of CXTA and DXA measurements, T-scores can be used to interpret the findings as in DXA [40]. Per ACRad practice parameters, in

premenopausal women, men younger than 50, and children Z-scores are used, with a Z-score of less or equal to  $-2.0$  considered to be below the expected range for age.

QCT is beneficial for some rheumatological disorders such as AS and DISH. For example, a study comparing DXA and QCT in older men with DISH demonstrated that QCT was better suited to differentiate men with and without vertebral fractures [8]. Another study comparing DXA and QCT in AS found that with QCT, a decrease in vertebral trabecular bone density could already be observed in the initial disease stages and that in advanced ankyloses in the vertebral region (substantial syndesmophytes), QCT was superior to document bone loss [41]. It has also been shown that trabecular measurements of spine BMD using QCT are not influenced by osteoarthritis of the spine and that in patients with advanced osteoarthritis, QCT may be superior to DXA [42]. Figure 2 shows a QCT study of a patient with rheumatoid arthritis, a severe T12 fracture, and osteoporotic BMD at the lumbar spine.

## Quantitative Ultrasound

QUS is an inexpensive, nonionizing technique which is typically performed at peripheral regions such as the forearm or calcaneus. The literature supports QUS as a predictor of fracture risk in osteoporotic populations, and further suggests that QUS may provide information on bone quality beyond simple bone mass [43, 44]. In a recent study of 60 normal adults, a US derived bone measurement correlated well to DXA derived BMD at the 1/3 region of the distal radius [45]. The device used in this study was recently granted FDA approval for clinical use. QUS continues to be limited by a lack of standardization, both in terms of technology and technical parameters evaluated (e.g., broadband ultrasound attenuation, speed of sound, stiffness index, amplitude-dependent speed of sound, and bone transmission time) and anatomic sites evaluated (e.g., calcaneus, tibia, radius, phalanges) [46]. However, if DXA is not available or cannot be done, the ISCD official position is that pharmacologic treatment can be initiated if fracture probability, using device-specific thresholds and in conjunction with clinical risk factors, is sufficiently high ([www.iscd.org/official-positions/2019-iscd-official-positions-adult](http://www.iscd.org/official-positions/2019-iscd-official-positions-adult)).

A recent meta-analysis conducted to assess the role of QUS in inflammatory rheumatic diseases came to the conclusion that the current literature does not support the substitution of QUS for DXA in the diagnosis and monitoring of osteoporosis in rheumatic diseases [47]. For rheumatoid arthritis, the authors stated that QUS has a moderate to strong correlation with DXA and good discriminatory performance in differentiating osteoporotic individuals and controls, but conflicting data were found on the use of QUS in the early disease process and in corticosteroid-induced osteoporosis [47].

## Diagnostic Techniques to Measure Bone Quality

As evidence has emerged that additional factors beyond BMD are important in the evaluation of bone health and fracture risk, diagnostic techniques to measure bone quality have been developed and validated. However, compared with standardized BMD



measurements, which are part of clinical routine, clinical bone quality evaluations are still in development and, for the most part, remain research tools.

Some of these diagnostic techniques use advanced analysis tools based on three-dimensional imaging modalities (such as HR-pQCT, MD-CT, and MRI) that have been developed and optimized to quantify bone geometry, microstructure, and biomechanical parameters. The goal of these techniques is to more accurately predict fractures and more sensitively monitor therapeutic interventions.

## High-Resolution Peripheral Quantitative Computed Tomography

Introduced in 2004, HR-pQCT is a small-bore, high-resolution, dedicated extremity CT imaging system, currently available from a single manufacturer (Scanco Medical AG, Brüttisellen, Switzerland). In 15 years since its introduction, installation of HR-pQCT systems worldwide as well as the number of publications and the size of cohort studies has grown exponentially [48-51]. However, at this time, HR-pQCT remains a research tool without FDA approval for use as a clinical diagnostic tool. The first generation of the HR-pQCT (XtremeCT) was limited to imaging the distal leg and foot and the distal forearm and hand, and achieved a spatial resolution of 82  $\mu\text{m}$  (isotropic voxel dimension) in the standard in vivo scan setting, significantly higher than any other available in vivo imaging tool [52]. The newest generation of this device (XtremeCT II) has an improved spatial resolution of 61  $\mu\text{m}$ , and the ability to scan more proximally, including the knee [53]. Because it is limited to peripheral scan locations, the effective radiation dose of HR-pQCT is substantially lower compared with whole body CT and does not involve critical, radiosensitive organs. For a standard distal tibia or distal radius scan, effective dose is less than 5  $\mu\text{Sv}$ . For a full knee scan, which requires multiple image stacks, effective dose is less than 50  $\mu\text{Sv}$ .

The high resolution, volumetric acquisition protocol of HR-pQCT allows for quantification of volumetric bone mineral density, geometry, and microstructure of trabecular and cortical compartments. For the distal tibia and distal radius evaluation sites, a standard semiautomated segmentation and analysis protocol is provided by the manufacturer. This protocol requires operator oversight, and often manual correction, during the process of identifying periosteal and endocortical boundaries. Based on this semiautomated contouring and segmentation process, the trabecular and cortical compartments are identified for subsequent densitometric, morphometric, and biomechanical analyses. A calibration phantom containing a series of hydroxyapatite-polymer mixtures is scanned to generate a calibration curve in order to output volumetric BMD data in units of  $\text{mgHA}/\text{cm}^3$ . Volumetric BMD is reported for the whole bone as well as trabecular and cortical compartments individually. Within the trabecular compartment, morphometric indices describing trabecular thickness, number, separation, and heterogeneity, as well as connectivity, structure model index (a measure of the rod or plate-like appearance of the structure), and anisotropy are calculated. Within the cortical compartment, cortical thickness and porosity are calculated. For other anatomic sites—for example, the knee, hand, or foot—customized segmentation and analysis strategies have been developed [54, 55]. Of particular interest to the field of rheumatology, there are recent efforts by the Study Group for Xtreme-CT in Rheumatoid



Arthritis (SPECTRA) to define and standardize procedures for the evaluation of joint space width and bone erosions [56].

Finite element analysis (FEA) applied to volumetric HR-pQCT data is used to quantify biomechanical properties. Binarized bone volumes are converted to FEA models with operator-determined mechanical properties and failure criteria, and “virtually” loaded in uniaxial compression. Stiffness, elastic modulus, and estimated strength are calculated, as well as cortical load fraction, which indicates the proportion of load borne by the cortical vs. trabecular compartments [57]. These biomechanical models have been validated against mechanical testing in cadaver specimens [58]. HR-pQCT FEA-derived estimates of bone strength performed better than DXA-derived areal BMD at classifying women with and without prior fracture [59] and were shown to predict fracture independent of areal BMD in a prospective study [60].

Reproducibility of HR-pQCT densitometric measures is high, with coefficient of variation < 1%, while microstructural and biomechanical measures typically have a coefficient of variation of 4–5%, and up to ~ 13% for cortical porosity [57, 61-63].

Advanced analyses have been developed by the user community. Topological analyses including individual trabecular segmentation (ITS) [64] and cortical pore topology [65] have been applied to provide insight into microstructural alterations in response to aging and disease. Figure 3 depicts the ability of HR-pQCT imaging and cortical pore analysis to visualize and quantify the impact of 6 weeks of disuse on cortical bone porosity. Trabecular and cortical subregional analyses have been developed to provide spatially-resolved information [67]. Taking this to a more detailed level, statistical parametric mapping has been applied to HR-pQCT [68].

A number of clinical studies have demonstrated the utility of HR-pQCT measures in fracture prediction as well as monitoring of therapeutic intervention. In aging populations, cortical and trabecular microarchitecture [50] as well as volumetric BMD and biomechanical measures from FEA [69] have been shown to predict incident fracture independent of DXA areal BMD and clinical risk factors. In patients with rheumatoid arthritis, erosion volume, cortical interruptions, and microstructural parameters have been demonstrated to be sensitive metrics for the evaluation of treatment response [70].

There are several disadvantages of HR-pQCT; most notably that it is not approved for clinical use at this time. Additionally, it is limited to peripheral skeletal sites and therefore can provide no direct insight into bone quality at the lumbar spine or proximal femur—common sites for osteoporotic fragility fractures. Persistent issues include motion artifacts, which sometimes limit morphological analysis of bone microstructure [71], and a lack of consensus on imaging protocols, particularly in imaging children and adolescents [72, 73].

## Multi-Detector CT

MD-CT provides superior spatial resolution compared with traditional whole-body spiral CT scanners and is standard in clinical use. An advantage of MD-CT compared with HR-pQCT is access to central anatomic sites at greatest risk for fragility fractures, such as the spine and

proximal femur, where monitoring of disease and therapy may be most efficient. However, the radiation exposure required to achieve high spatial resolution and adequate image quality is substantial [9, 74]. Compared with the effective dose of HR-pQCT or an adult DXA spine exam (0.001–0.05 mSv) and that of a conventional QCT spine exam (0.06–0.3 mSv), the radiation exposure of a high-resolution MD-CT vertebral microstructure protocol is orders of magnitude higher (~ 3 mSv) [74, 75]. Importantly, low-dose MD-CT techniques are being developed, for example, iterative reconstruction algorithms or sparse sampling, which provide reduction in radiation exposure while maintaining high diagnostic accuracy [76, 77].

With slice thickness on the order of 500  $\mu\text{m}$  and in-plane resolution of ~ 150  $\mu\text{m}$ , imaging of trabecular or cortical microstructure with MD-CT is certainly limited and subject to substantial partial volume effects. However, for certain microstructural parameters obtained with MD-CT—in particular plate-rod ratio [78]—good correlations have been achieved with values obtained from gold standard microCT images [79].

Clinical studies have demonstrated the utility of MD-CT in diagnosing existing fractures with high specificity and sensitivity [80]. Further, MD-CT-derived structure measures at the proximal femur and lumbar spine have been shown to improve differentiation of fracture patients from normal controls [81]. MD-CT was also shown to be well-suited for monitoring teriparatide-associated changes of vertebral microstructure [74]. Prediction of incident vertebral fracture has been demonstrated using MD-CT-based FEA [82].

## Magnetic Resonance Imaging

Advances in MRI software and hardware including 3T and 7T magnets and improved coil design have enabled improved skeletal structural imaging. Lack of radiation makes MRI attractive for both clinical and scientific studies. However, historically, the technique has been used mainly for peripheral imaging. Recent advances in image acquisition have resulted in improved image quality even at central sites. At the proximal femur—a particularly challenging site due to the soft tissue around the femur and thus large distance from the radiofrequency coil to the femur—depiction of trabecular structure with minimal blurring and high SNR efficiency has been achieved (Fig. 4) [83, 84]. Calibration and validation studies have demonstrated that MR-derived trabecular structure measures correlate with histology, microCT, and biomechanical strength derived from in vitro studies [85–88]. MRI-based texture measures are also used to represent bone quality [89]. MRI texture analysis quantifies the organizational pattern of pixel grayscales representing the underlying tissue; the spatial distribution of grayscales can reflect the structural properties of the imaged tissue. This approach is similar to TBS from DXA; however, rather than using low resolution projectional DXA data, in MRI-based texture analysis, results are derived from three-dimensional image volumes with high anatomic detail.

Over the last decade, technical advancements in MRI acquisition have enabled visualization as well as microstructural and compositional analysis of cortical bone, previously impossible with standard MRI acquisition. This has been accomplished using ultra-short echo time (UTE) imaging. UTE imaging allows detection of signal components with T2 relaxation times on the order of a few hundred microseconds. In bone, this signal is derived from “free

water” residing in the osteonal and lacuno-cannalicular networks and from “bound water” within the bone matrix [90]. Techawiboonwong et al. validated bone water imaging (i.e., the measurement of water in cortical bone) using a UTE sequence in cortical bone specimens and studied the tibial midshaft in premenopausal and postmenopausal females and patients on hemodialysis [91]. The quantitative analysis showed that bone water content was 135% higher in the patients on maintenance dialysis than in the premenopausal women and 43% higher than in the postmenopausal women. Because bone water exists primarily in the pore system of cortical bone, bone water content is thought to provide a surrogate measure for cortical porosity. Accordingly, the bone water content results align with the expected porosity differences in these three populations. More recently, Rajapaske et al. presented a calculation method and validation of a metric-termed porosity index. In *ex vivo* bone specimens, porosity index was well correlated with microCT-based porosity quantification [92].

Despite these advancements in MRI bone imaging, numerous challenges remain. Spatial resolution remains above the range of trabecular and cortical microstructural dimensions (resolution in plane 0.15–0.3 mm<sup>2</sup>, slice thickness 0.3–1 mm). Partial volume artifacts due to limited resolution combined with susceptibility artifacts result in systematic bias in structure parameter values; in particular, the morphological parameter trabecular bone volume fraction and trabecular thickness were demonstrated to exhibit large discrepancies compared with HR-pQCT (MR/HR-pQCT = 3–4) [52]. In addition, long acquisition times make MRI susceptible to motion artifacts, which negatively impact structural analysis.

MRI-derived bone quality measures have been shown to provide additional information to BMD in differentiating individuals with and without fragility fractures [93-97]. Longitudinal studies using MRI-derived trabecular microarchitecture measures have demonstrated the feasibility of the technique in monitoring the effect of therapeutic interventions [98] [99]. Folkesson et al. found longitudinal changes in MR-derived bone microarchitecture due to bisphosphonate therapy in perimenopausal women treated for 24 months with alendronate [100]. In a prospective longitudinal study of a cohort undergoing high tibial osteotomy, MRI was used to quantify changes in subchondral bone following surgery, finding both a reversal of previous subchondral abnormalities and a positive association of this subchondral structural normalization with functional outcome [101].

## Conclusion

Patients with inflammatory rheumatological disorders have a high rate of fragility fractures. Diagnostic assessment of bone density and quality is therefore critically important. The standard assessment tool is DXA and though it does have some limitations, it provides a good general assessment, which can be augmented through VFA and TBS measurements. QCT is more of a problem solver in particular in patients with AS and DISH and though similar in diagnostic performance as DXA, it is not as frequently used anymore. Newer techniques to assess bone quality have a role in helping to better characterize bone fragility in areas where bone density has limitations, such as in patients with corticosteroid therapy, but they are currently not a clinical standard.

## References

Papers of particular interest, published recently, have been highlighted as:

- Of importance

1. Xue AL, Wu SY, Jiang L, Feng AM, Guo HF, Zhao P. Bone fracture risk in patients with rheumatoid arthritis: a meta-analysis. *Medicine (Baltimore)*. 2017;96(36):e6983 [PubMed: 28885321] This meta-analysis shows well that both male and female patients with rheumatoid arthritis have a significantly higher fracture risk, in particular vertebral and hip fractures.
2. Dubrovsky AM, Lim MJ, Lane NE. Osteoporosis in rheumatic diseases: anti-rheumatic drugs and the skeleton. *Calcif Tissue Int*. 2018;102(5):607–18 [PubMed: 29470611] This review article documents that medications approved for the treatment of osteoporosis, including denosumab, cathepsin K, bisphosphonates, anti-sclerostin antibodies and parathyroid hormone (hPTH 1–34), have efficacy in both the prevention of systemic bone loss and reducing localized bone erosions.
3. Confavreux CB, Chapurlat RD. Systemic bone effects of biologic therapies in rheumatoid arthritis and ankylosing spondylitis. *Osteoporos Int*. 2011;22(4):1023–36. [PubMed: 20959960]
4. Paggiosi MA, Peel NF, Eastell R. The impact of glucocorticoid therapy on trabecular bone score in older women. *Osteoporos Int*. 2015;26(6):1773–80. [PubMed: 25743176]
5. Martel D, Laporq B, Saxena A, Belmont HM, Turyan G, Honig S, et al. 3T chemical shift-encoded MRI: detection of altered proximal femur marrow adipose tissue composition in glucocorticoid users and validation with magnetic resonance spectroscopy. *J Magn Reson Imaging*. 2019;50(2):490–6. [PubMed: 30548522]
6. Magrey MN, Lewis S, Asim Khan M. Utility of DXA scanning and risk factors for osteoporosis in ankylosing spondylitis-a prospective study. *Semin Arthritis Rheum*. 2016;46(1):88–94. [PubMed: 27162010]
7. Nigil Haroon N, Szabo E, Raboud JM, McDonald-Blumer H, Fung L, Josse RG, et al. Alterations of bone mineral density, bone microarchitecture and strength in patients with ankylosing spondylitis: a cross-sectional study using high-resolution peripheral quantitative computerized tomography and finite element analysis. *Arthritis Res Ther*. 2015;17:377. [PubMed: 26704700]
8. Diederichs G, Engelken F, Marshall LM, Peters K, Black DM, Issever AS, et al. Diffuse idiopathic skeletal hyperostosis (DISH): relation to vertebral fractures and bone density. *Osteoporos Int*. 2011;22(6):1789–97. [PubMed: 20882271]
9. Damilakis J, Adams JE, Guglielmi G, Link TM. Radiation exposure in X-ray-based imaging techniques used in osteoporosis. *Eur Radiol*. 2011;20(11):2707–14.
10. Tothill P, Hannan WJ. Precision and accuracy of measuring changes in bone mineral density by dual-energy X-ray absorptiometry. *Osteoporos Int*. 2007;18(11):1515–23. [PubMed: 17483864]
11. WHO, editor. Technical Report: Assessment of fracture risk and its application to screening for postmenopausal osteoporosis: a report of a WHO study group. Geneva: World Health Organization; 1994.
12. Baim S, Binkley N, Bilezikian JP, Kendler DL, Hans DB, Lewiecki EM, et al. Official positions of the International Society for Clinical Densitometry and executive summary of the 2007 ISCD Position Development Conference. *J Clin Densitom*. 2008;11(1):75–91. [PubMed: 18442754]
13. Lewiecki EM, Baim S, Langman CB, Bilezikian JP. The official positions of the International Society for Clinical Densitometry: perceptions and commentary. *J Clin Densitom*. 2009;12(3):267–71. [PubMed: 19546020]
14. Lewiecki EM, Gordon CM, Baim S, Binkley N, Bilezikian JP, Kendler DL, et al. Special report on the 2007 adult and pediatric Position Development Conferences of the International Society for Clinical Densitometry. *Osteoporos Int*. 2008;19(10):1369–78. [PubMed: 18633664]
15. Gluer CC. Monitoring skeletal changes by radiological techniques. *J Bone Miner Res*. 1999;14(11):1952–62. [PubMed: 10571696]
16. Humbert L, Martelli Y, Fonolla R, Steghofer M, Di Gregorio S, Malouf J, et al. 3D-DXA: assessing the femoral shape, the trabecular macrostructure and the cortex in 3D from DXA images. *IEEE Trans Med Imaging*. 2017;36(1):27–39. [PubMed: 27448343]

17. Vaananen SP, Grassi L, Flivik G, Jurvelin JS, Isaksson H. Generation of 3D shape, density, cortical thickness and finite element mesh of proximal femur from a DXA image. *Med Image Anal.* 2015;24(1):125–34. [PubMed: 26148575]
18. Arabi A, Baddoura R, Awada H, Khoury N, Haddad S, Ayoub G, et al. Discriminative ability of dual-energy X-ray absorptiometry site selection in identifying patients with osteoporotic fractures. *Bone.* 2007;40(4):1060–5. [PubMed: 17223616]
19. Kanis JA. Diagnosis of osteoporosis and assessment of fracture risk. *Lancet.* 2002;359(9321):1929–36. [PubMed: 12057569]
20. Maricic M Use of DXA-based technology for detection and assessment of risk of vertebral fracture in rheumatology practice. *Curr Rheumatol Rep.* 2014;16(8):436. [PubMed: 24938441]
21. Siris ES, Chen YT, Abbott TA, Barrett-Connor E, Miller PD, Wehren LE, et al. Bone mineral density thresholds for pharmacological intervention to prevent fractures. *Arch Intern Med.* 2004;164(10):1108–12. [PubMed: 15159268]
22. Kanis JA, Johansson H, Oden A, Dawson-Hughes B, Melton LJ 3rd, McCloskey EV The effects of a FRAX revision for the USA. *Osteoporos Int.* 2009;21(1):35–40. [PubMed: 19705047]
23. Kanis JA, Johnell O, Oden A, Johansson H, McCloskey E. FRAX and the assessment of fracture probability in men and women from the UK. *Osteoporos Int.* 2008;19(4):385–97. [PubMed: 18292978]
24. Kanis JA, Oden A, Johansson H, Borgstrom F, Strom O, McCloskey E. FRAX and its applications to clinical practice. *Bone.* 2009;44(5):734–43. [PubMed: 19195497]
25. Link TM. Radiology of osteoporosis. *Can Assoc Radiol J.* 2016;67(1):28–40. [PubMed: 26105503]
26. Expert Panel on Musculoskeletal I, Ward RJ, Roberts CC, Bencardino JT, Arnold E, Baccei SJ, et al. ACR appropriateness criteria((R)) osteoporosis and bone mineral density. *J Am Coll Radiol.* 2017;14(5S):S189–202. [PubMed: 28473075]
27. Link TM. Screening: assessing bone structure in the prediction of osteoporotic fractures. *Nat Rev Rheumatol.* 2012;8(1):6–8.
28. Silva BC, Leslie WD, Resch H, Lamy O, Lesnyak O, Binkley N, et al. Trabecular bone score: a noninvasive analytical method based upon the DXA image. *J Bone Miner Res.* 2014;29(3):518–30. [PubMed: 24443324]
29. Bousson V, Bergot C, Sutter B, Levitz P, Cortet B, Scientific Committee of the Groupe de Recherche et d'Information sur les O. Trabecular bone score (TBS): available knowledge, clinical relevance, and future prospects. *Osteoporos Int.* 2012;23(5):1489–501. [PubMed: 22083541]
30. Leib E, Winzenrieth R, Lamy O, Hans D. Comparing bone microarchitecture by trabecular bone score (TBS) in Caucasian American women with and without osteoporotic fractures. *Calcif Tissue Int.* 2014;95(3):201–8. [PubMed: 24948332]
31. Hans D, Barthe N, Boutroy S, Pothuau L, Winzenrieth R, Krieg MA. Correlations between trabecular bone score, measured using anteroposterior dual-energy x-ray absorptiometry acquisition, and 3-dimensional parameters of bone microarchitecture: an experimental study on human cadaver vertebrae. *J Clin Densitom.* 2011;14(3):302–12. [PubMed: 21724435]
32. Boutroy S, Hans D, Sornay-Rendu E, Vilayphiou N, Winzenrieth R, Chapurlat R. Trabecular bone score improves fracture risk prediction in non-osteoporotic women: the OFELY study. *Osteoporos Int.* 2013;24(1):77–85. [PubMed: 23070481]
33. Arterburn DE, Olsen MK, Smith VA, Livingston EH, Van Scoyoc L, Yancy WS Jr, et al. Association between bariatric surgery and long-term survival. *JAMA.* 2015;313(1):62–70. [PubMed: 25562267]
34. McCloskey EV, Oden A, Harvey NC, Leslie WD, Hans D, Johansson H, et al. A meta-analysis of trabecular bone score in fracture risk prediction and its relationship to FRAX. *J Bone Miner Res.* 2016;31(5):940–8. [PubMed: 26498132]
35. Martineau P, Leslie WD, Johansson H, Harvey NC, McCloskey EV, Hans D, et al. In which patients does lumbar spine trabecular bone score (TBS) have the largest effect? *Bone.* 2018;113:161–8. [PubMed: 29802962]
36. Breban S, Briot K, Kolta S, Paternotte S, Ghazi M, Fechtenbaum J, et al. Identification of rheumatoid arthritis patients with vertebral fractures using bone mineral density and trabecular bone score. *J Clin Densitom.* 2012;15(3):260–6. [PubMed: 22445857]

37. Carey JJ, Buehring B. Current imaging techniques in osteoporosis. *Clin Exp Rheumatol*. 2018;36(Suppl 114(5)):115–26.
38. Cheung AM, McKenna MJ, van de Laarschot DM, Zillikens MC, Peck V, Srighanthan J, et al. The Official Positions of the International Society for Clinical Densitometry: detection of atypical femur fractures. *J Clin Densitom*. 2019.
39. Black DM, Greenspan SL, Ensrud KE, Palermo L, McGowan JA, Lang TF, et al. The effects of parathyroid hormone and alendronate alone or in combination in postmenopausal osteoporosis. *N Engl J Med*. 2003;349(13):1207–15. [PubMed: 14500804]
40. Link TM, Lang TF. Axial QCT: clinical applications and new developments. *J Clin Densitom*. 2014.
41. Lange U, Kluge A, Strunk J, Teichmann J, Bachmann G. Ankylosing spondylitis and bone mineral density-what is the ideal tool for measurement? *Rheumatol Int*. 2005;26(2):115–20. [PubMed: 15538574]
42. Guglielmi G, Floriani I, Torri V, Li J, van Kuijk C, Genant HK, et al. Effect of spinal degenerative changes on volumetric bone mineral density of the central skeleton as measured by quantitative computed tomography. *Acta Radiol*. 2005;46(3):269–75. [PubMed: 15981723]
43. Gluer CC. Quantitative ultrasound-it is time to focus research efforts. *Bone*. 2007;40(1):9–13. [PubMed: 16949359]
44. Moayyeri A, Adams JE, Adler RA, Krieg MA, Hans D, Compston J, et al. Quantitative ultrasound of the heel and fracture risk assessment: an updated meta-analysis. *Osteoporos Int*. 2012;23(1):143–53. [PubMed: 22037972]
45. Stein EM, Rosete F, Young P, Kamanda-Kosseh M, McMahan DJ, Luo G, et al. Clinical assessment of the 1/3 radius using a new desktop ultrasonic bone densitometer. *Ultrasound Med Biol*. 2013;39(3):388–95. [PubMed: 23312957]
46. Krieg MA, Barkmann R, Gonnelli S, Stewart A, Bauer DC, Del Rio BL, et al. Quantitative ultrasound in the management of osteoporosis: the 2007 ISCD Official Positions. *J Clin Densitom*. 2008;11(1):163–87. [PubMed: 18442758]
47. Oo WM, Naganathan V, Bo MT, Hunter DJ. Clinical utilities of quantitative ultrasound in osteoporosis associated with inflammatory rheumatic diseases. *Quant Imaging Med Surg*. 2018;8(1):100–13 [PubMed: 29541626] This review article shows that although Quantitative Ultrasound may have some complementary benefits to fracture risk prediction models, current literature does not support the substitution of Quantitative Ultrasound for DXA in the diagnosis and monitoring of osteoporosis in the rheumatic diseases.
48. Burt LA, Manske SL, Hanley DA, Boyd SK. Lower bone density, impaired microarchitecture, and strength predict future fragility fracture in postmenopausal women: 5-year follow-up of the Calgary CaMos cohort. *J Bone Miner Res*. 2018;33(4):589–97. [PubMed: 29363165]
49. Chapurlat R, Pialat JB, Merle B, Confavreux E, Duvert F, Fontanges E, et al. The QUALYOR (Qualite Osseuse LYon Orleans) study: a new cohort for non invasive evaluation of bone quality in postmenopausal osteoporosis. Rationale and study design. *Arch Osteoporos*. 2017;13(1):2. [PubMed: 29282548]
50. Samelson EJ, Broe KE, Xu H, Yang L, Boyd S, Biver E, et al. Cortical and trabecular bone microarchitecture as an independent predictor of incident fracture risk in older women and men in the bone microarchitecture international consortium (BoMIC): a prospective study. *Lancet Diabetes Endocrinol*. 2019;7(1):34–43. [PubMed: 30503163]
51. Vranken L, Wyers CE, van Rietbergen B, Driessen JHM, Geusens P, Janzing HMJ, et al. The association between prevalent vertebral fractures and bone quality of the distal radius and distal tibia as measured with HR-pQCT in postmenopausal women with a recent non-vertebral fracture at the Fracture Liaison Service. *Osteoporos Int*. 2019;30(9):1789–97. [PubMed: 31312863]
52. Kazakia GJ, Hyun B, Burghardt AJ, Krug R, Newitt DC, de Papp AE, et al. In vivo determination of bone structure in postmenopausal women: a comparison of HR-pQCT and high-field MR imaging. *J Bone Miner Res*. 2008;23(4):463–74. [PubMed: 18052756]
53. Kroker A, Zhu Y, Manske SL, Barber R, Mohtadi N, Boyd SK. Quantitative in vivo assessment of bone microarchitecture in the human knee using HR-pQCT. *Bone*. 2017;97:43–8. [PubMed: 28039095]



54. Michalak GJ, Walker R, Boyd SK. Concurrent assessment of cartilage morphology and bone microarchitecture in the human knee using contrast-enhanced HR-pQCT imaging. *J Clin Densitom.* 2019;22(1):74–85. [PubMed: 30120027]
55. Sada K, Chiba K, Kajiyama S, Okazaki N, Yonekura A, Tomita M, et al. Bone mineral density and microstructure of the elbow in baseball pitchers: an analysis by second-generation HR-pQCT. *J Clin Densitom.* 2019.
56. Barnabe C, Feehan L, Spectra. High-resolution peripheral quantitative computed tomography imaging protocol for metacarpophalangeal joints in inflammatory arthritis: the SPECTRA collaboration. *J Rheumatol.* 2012;39(7):1494–5. [PubMed: 22753808]
57. Burghardt AJ, Buie HR, Laib A, Majumdar S, Boyd SK. Reproducibility of direct quantitative measures of cortical bone microarchitecture of the distal radius and tibia by HR-pQCT. *Bone.* 2010;47(3):519–28. [PubMed: 20561906]
58. Mueller DK, Kutscherenko A, Bartel H, Vlassenbroek A, Ourednicek P, Erckenbrecht J. Phantomless QCT BMD system as screening tool for osteoporosis without additional radiation. *Eur J Radiol.* 2011;79(3):375–81. [PubMed: 20223609]
59. Nishiyama KK, Macdonald HM, Hanley DA, Boyd SK. Women with previous fragility fractures can be classified based on bone microarchitecture and finite element analysis measured with HR-pQCT. *Osteoporos Int.* 2013;24(5):1733–40. [PubMed: 23179565]
60. Sornay-Rendu E, Boutroy S, Duboeuf F, Chapurlat RD. Bone microarchitecture assessed by HR-pQCT as predictor of fracture risk in postmenopausal women: the OFELY study. *J Bone Miner Res.* 2017;32(6):1243–51. [PubMed: 28276092]
61. Boutroy S, Bouxsein ML, Munoz F, Delmas PD. In vivo assessment of trabecular bone microarchitecture by high-resolution peripheral quantitative computed tomography. *J Clin Endocrinol Metab.* 2005;90(12):6508–15. [PubMed: 16189253]
62. Chiba K, Okazaki N, Kurogi A, Isobe Y, Yonekura A, Tomita M, et al. Precision of second-generation high-resolution peripheral quantitative computed tomography: intra- and intertester reproducibilities and factors involved in the reproducibility of cortical porosity. *J Clin Densitom.* 2018;21(2):295–302. [PubMed: 28256308]
63. MacNeil JA, Boyd SK. Improved reproducibility of high-resolution peripheral quantitative computed tomography for measurement of bone quality. *Med Eng Phys.* 2008;30(6):792–9. [PubMed: 18164643]
64. Zhou B, Zhang Z, Wang J, Yu YE, Liu XS, Nishiyama KK, et al. In vivo precision of digital topological skeletonization based individual trabecula segmentation (ITS) analysis of trabecular microstructure at the distal radius and tibia by HR-pQCT. *Pattern Recogn Lett.* 2016;76:83–9.
65. Tjong W, Nirody J, Burghardt AJ, Carballido-Gamio J, Kazakia GJ. Structural analysis of cortical porosity applied to HR-pQCT data. *Med Phys.* 2014;41(1):013701. [PubMed: 24387533]
66. Kazakia GJ, Tjong W, Nirody JA, Burghardt AJ, Carballido-Gamio J, Patsch JM, et al. The influence of disuse on bone microstructure and mechanics assessed by HR-pQCT. *Bone.* 2014;63:132–40. [PubMed: 24603002]
67. Sode M, Burghardt AJ, Kazakia GJ, Link TM, Majumdar S. Regional variations of gender-specific and age-related differences in trabecular bone structure of the distal radius and tibia. *Bone.* 2010;46(6):1652–60. [PubMed: 20188877]
68. Carballido-Gamio J, Bonaretti S, Kazakia GJ, Khosla S, Majumdar S, Lang TF, et al. Statistical parametric mapping of HR-pQCT images: a tool for population-based local comparisons of micro-scale bone features. *Ann Biomed Eng.* 2017;45(4):949–62. [PubMed: 27830488]
69. Langsetmo L, Peters KW, Burghardt AJ, Ensrud KE, Fink HA, Cawthon PM, et al. Volumetric bone mineral density and failure load of distal limbs predict incident clinical fracture independent HR-pQCT BMD and failure load predicts incident clinical fracture of FRAX and clinical risk factors among older men. *J Bone Miner Res.* 2018;33(7):1302–11. [PubMed: 29624722]
70. Shimizu T, Choi HJ, Heilmeyer U, Tanaka M, Burghardt AJ, Gong J, et al. Assessment of 3-month changes in bone microstructure under anti-TNFalpha therapy in patients with rheumatoid arthritis using high-resolution peripheral quantitative computed tomography (HR-pQCT). *Arthritis Res Ther.* 2017;19(1):222. [PubMed: 28978352]



71. Pialat JB, Burghardt AJ, Sode M, Link TM, Majumdar S. Visual grading of motion induced image degradation in high resolution peripheral computed tomography: impact of image quality on measures of bone density and micro-architecture. *Bone*. 2012;50(1):111–8. [PubMed: 22019605]
72. Gordon CM, Leonard MB, Zemel BS. International Society for Clinical D. 2013 Pediatric Position Development Conference: executive summary and reflections. *J Clin Densitom*. 2014;17(2):219–24. [PubMed: 24657108]
73. Vierge M, Preka E, Ginhoux T, Chapurlat R, Ranchin B, Bacchetta J. Pediatric bone evaluation with HR-pQCT: a comparison between standard and height-adjusted positioning protocols in a cohort of teenagers with chronic kidney disease. *Arch Pediatr*. 2019;26(3):151–7. [PubMed: 30827777]
74. Graeff C, Timm W, Nickelsen TN, Farrerons J, Marin F, Barker C, et al. Monitoring teriparatide-associated changes in vertebral microstructure by high-resolution CT in vivo: results from the EUROFORs study. *J Bone Miner Res*. 2007;22(9):1426–33. [PubMed: 17547537]
75. Ito M, Ikeda K, Nishiguchi M, Shindo H, Uetani M, Hosoi T, et al. Multi-detector row CT imaging of vertebral microstructure for evaluation of fracture risk. *J Bone Miner Res*. 2005;20(10):1828–36. [PubMed: 16160740]
76. Lee SH, Yun SJ, Kim DH, Jo HH, Song JG, Park YS. Diagnostic usefulness of low-dose lumbar multi-detector CT with iterative reconstruction in trauma patients: a comparison with standard dose CT. *Br J Radiol*. 2017;90(1077):20170181. [PubMed: 28707527]
77. Weinrich JM, Well L, Regier M, Behzadi C, Sehner S, Adam G, et al. MDCT in suspected lumbar spine fracture: comparison of standard and reduced dose settings using iterative reconstruction. *Clin Radiol*. 2018;73(7):675 e9–e15.
78. Saha PK, Liu Y, Chen C, Jin D, Letuchy EM, Xu Z, et al. Characterization of trabecular bone plate-rod microarchitecture using multirow detector CT and the tensor scale: algorithms, validation, and applications to pilot human studies. *Med Phys*. 2015;42(9):5410–25. [PubMed: 26328990]
79. Chen C, Zhang X, Guo J, Jin D, Letuchy EM, Burns TL, et al. Quantitative imaging of peripheral trabecular bone microarchitecture using MDCT. *Med Phys*. 2018;45(1):236–49. [PubMed: 29064579]
80. Alabousi M, Gauthier ID, Li N, Dos Santos GM, Golev D, Atlas MN, et al. Multi-detector CT for suspected hip fragility fractures: a diagnostic test accuracy systematic review and meta-analysis. *Emerg Radiol*. 2019;26(5):549–56. [PubMed: 31209592]
81. Rodriguez-Soto AE, Fritscher KD, Schuler B, Issever AS, Roth T, Kamelger F, et al. Texture analysis, bone mineral density, and cortical thickness of the proximal femur: fracture risk prediction. *J Comput Assist Tomogr*. 2010;34(6):949–57. [PubMed: 21084915]
82. Allaire BT, Lu D, Johannesdottir F, Kopperdahl D, Keaveny TM, Jarraya M, et al. Prediction of incident vertebral fracture using CT-based finite element analysis. *Osteoporos Int*. 2019;30(2):323–31. [PubMed: 30306225]
83. Chang G, Deniz CM, Honig S, Egol K, Regatte RR, Zhu Y, et al. MRI of the hip at 7T: feasibility of bone microarchitecture, high-resolution cartilage, and clinical imaging. *J Magn Reson Imaging*. 2014;39(6):1384–93. [PubMed: 24115554]
84. Han M, Chiba K, Banerjee S, Carballido-Gamio J, Krug R. Variable flip angle three-dimensional fast spin-echo sequence combined with outer volume suppression for imaging trabecular bone structure of the proximal femur. *J Magn Reson Imaging*. 2015;41(5):1300–10. [PubMed: 24956149]
85. Link T, Majumdar S, Lin J, Newitt D, Augat P, Ouyang X, et al. A comparative study of trabecular bone properties in the spine and femur using high resolution MRI and CT. *J Bone Miner Res*. 1998;13:122–32. [PubMed: 9443798]
86. Link TM, Vieth V, Langenberg R, Meier N, Lotter A, Newitt D, et al. Structure analysis of high resolution magnetic resonance imaging of the proximal femur: in vitro correlation with biomechanical strength and BMD. *Calcif Tissue Int*. 2003;72(2):156–65. [PubMed: 12370799]
87. Majumdar S, Kothari M, Augat P, Newitt DC, Link TM, Lin JC, et al. High-resolution magnetic resonance imaging: three-dimensional trabecular bone architecture and biomechanical properties. *Bone*. 1998;22(5):445–54. [PubMed: 9600777]

88. Phan CM, Matsuura M, Bauer JS, Dunn TC, Newitt D, Lochmueller EM, et al. Trabecular bone structure of the calcaneus: comparison of MR imaging at 3.0 and 1.5 T with micro-CT as the standard of reference. *Radiology*. 2006;239(2):488–96. [PubMed: 16569786]
89. Harrison LC, Nikander R, Sikio M, Luukkaala T, Helminen MT, Ryymin P, et al. MRI texture analysis of femoral neck: detection of exercise load-associated differences in trabecular bone. *J Magn Reson Imaging*. 2011;34(6):1359–66. [PubMed: 21954096]
90. Ma YJ, Chang EY, Bydder GM, Du J. Can ultrashort-TE (UTE) MRI sequences on a 3-T clinical scanner detect signal directly from collagen protons: freeze-dry and D2 O exchange studies of cortical bone and Achilles tendon specimens. *NMR Biomed*. 2016;29(7):912–7. [PubMed: 27148693]
91. Techawiboonwong A, Song HK, Leonard MB, Wehrli FW. Cortical bone water: in vivo quantification with ultrashort echotime MR imaging. *Radiology*. 2008;248(3):824–33. [PubMed: 18632530]
92. Rajapakse CS, Bashoor-Zadeh M, Li C, Sun W, Wright AC, Wehrli FW. Volumetric cortical bone porosity assessment with MR imaging: validation and clinical feasibility. *Radiology*. 2015;276(2):526–35. [PubMed: 26203710]
93. Cortet B, Boutry N, Dubois P, Bourel P, Cotten A, Marchandise X. In vivo comparison between computed tomography and magnetic resonance image analysis of the distal radius in the assessment of osteoporosis. *J Clin Densitom*. 2000;3:15–26. [PubMed: 10917740]
94. Link T, Majumdar S, Augat P, Lin J, Newitt D, Lu Y, et al. In vivo high resolution MRI of the calcaneus: differences in trabecular structure in osteoporosis patients. *J Bone Miner Res*. 1998;13:1175–82. [PubMed: 9661082]
95. Majumdar S, Link TM, Augat P, Lin JC, Newitt D, Lane NE, et al. Trabecular bone architecture in the distal radius using magnetic resonance imaging in subjects with fractures of the proximal femur. *Magnetic Resonance Science Center and Osteoporosis and Arthritis Research Group. Osteoporos Int* 1999;10(3):231–9. [PubMed: 10525716]
96. Wehrli F, Gomberg B, Saha P, Song H, Hwang S, Snyder P. Digital topological analysis of in vivo magnetic resonance microimages of trabecular bone reveals structural implications of osteoporosis. *J Bone Miner Res*. 2001;16:1520–31. [PubMed: 11499875]
97. Wehrli FW, Leonard MB, Saha PK, Gomberg BR. Quantitative high-resolution magnetic resonance imaging reveals structural implications of renal osteodystrophy on trabecular and cortical bone. *J Magn Reson Imaging*. 2004;20(1):83–9. [PubMed: 15221812]
98. Benito M, Gomberg B, Wehrli FW, Weening RH, Zemel B, Wright AC, et al. Deterioration of trabecular architecture in hypogonadal men. *J Clin Endocrinol Metab*. 2003;88(4):1497–502. [PubMed: 12679429]
99. Chesnut CH 3rd, Majumdar S, Newitt DC, Shields A, Van Pelt J, Laschansky E, et al. Effects of salmon calcitonin on trabecular microarchitecture as determined by magnetic resonance imaging: results from the QUEST study. *J Bone Miner Res*. 2005;20(9):1548–61. [PubMed: 16059627]
100. Folkesson J, Goldenstein J, Carballido-Gamio J, Kazakia G, Burghardt AJ, Rodriguez A, et al. Longitudinal evaluation of the effects of alendronate on MRI bone microarchitecture in postmenopausal osteopenic women. *Bone*. 2010;48(3):611–21. [PubMed: 21059422]
101. Gersing AS, Jungmann PM, Schwaiger BJ, Zarnowski J, Kopp FK, Landwehr S, et al. Longitudinal changes in subchondral bone structure as assessed with MRI are associated with functional outcome after high tibial osteotomy. *J ISAKOS*. 2018;3(4):205–12. [PubMed: 30705762]

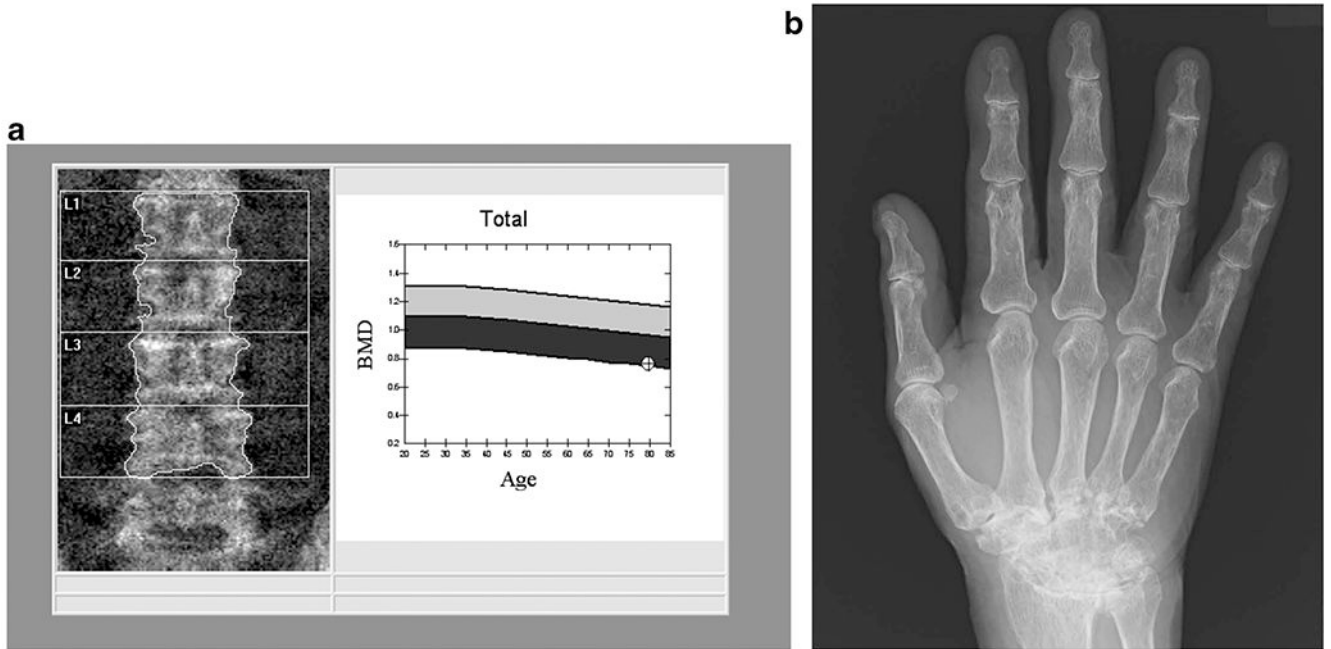


**Fig. 1.** 79-year-old man with a 25-year history of rheumatoid arthritis (RA). The DXA image of the lumbar spine (**a**) shows mild multilevel degenerative changes. A BMD of 0.762 g/cm<sup>2</sup> was measured, which corresponds to a T-score of -3.0. The radiograph of the right hand (**b**) shows advanced fusion of the carpal bones consistent with the long history of RA

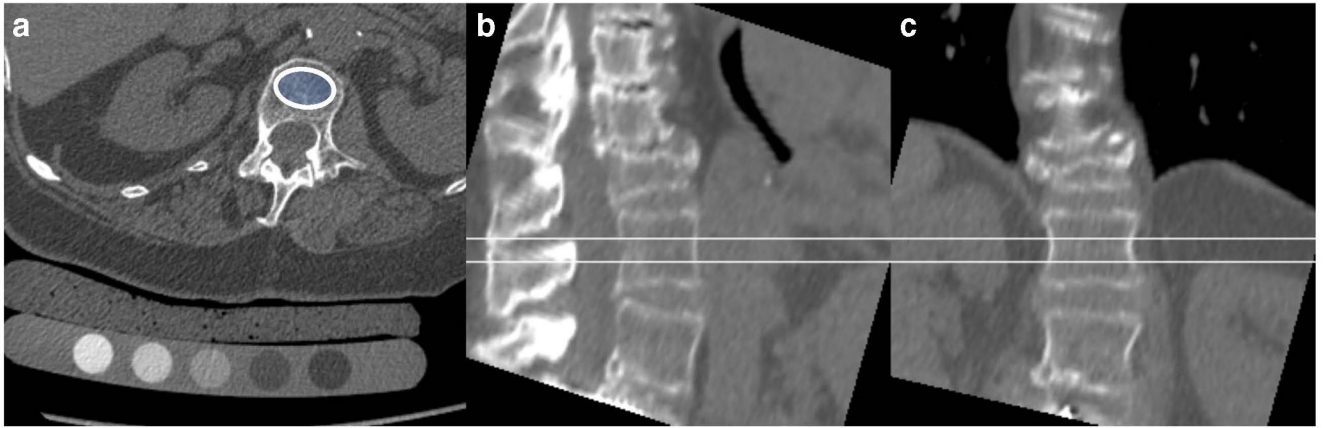


**Fig. 2.** 74-year-old woman with a history of rheumatoid arthritis and severe fracture deformity of T12. A volumetric QCT is shown with an axial source image with the calibration phantom and an oval region of interest in the L1 vertebral body (**a**) as well as sagittal (**b**) and coronal (**c**) reconstructions demonstrating the volume that was measured. BMD in L1 was 68.6 mg/cc and L2 76.1 mg/cc consistent with osteoporotic BMD according to American College of Radiology practice guidelines

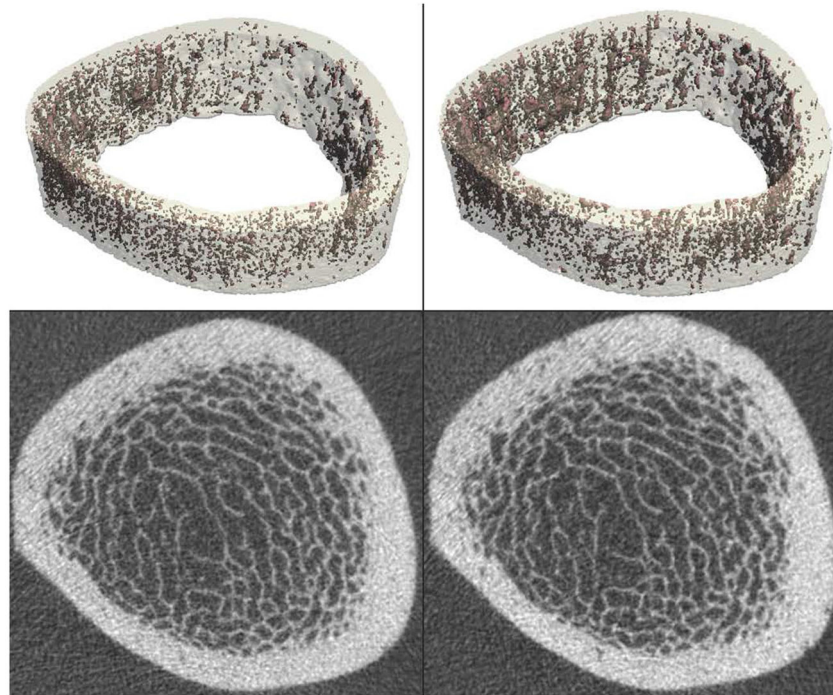


**Fig. 3.** Healthy 35-year-old male undergoing anterior cruciate ligament reconstruction and meniscus repair, instructed to remain non-weight-bearing for 6 weeks post-procedure. The distal tibia was imaged by HR-pQCT at two time points: just prior to surgery (left) and after 6 weeks of non-weight-bearing (right). Volumetric reconstructions of the cortical compartment, with porosity highlighted in red, are shown on the top row. Cross-sectional grayscale images are shown on the bottom row. HR-pQCT images and porosity analysis enable visualization and quantification of changes in bone microstructure over the 6-week disuse period [66]





**Fig. 4.** High-resolution MRI of the proximal femur in two postmenopausal women, one a healthy control (left) and one with osteoporosis and history of fragility fracture at a remote site (right). Courtesy of Roland Krug, PhD, UCSF